

Opto-Electrical Characterization of Erbium Doped Slot Waveguides

Andrea Tengattini^{a*}, Davide Gandolfi^a, Alessandro Marconi^a, Aleksei Anopchenko^a, Nikola Prtljaga^a, Joan Manel Ramirez^b, Federico Ferrarese Lupi^b, Yonder Berencen^b, Daniel Navarro Urrios^b, Blas Garrido^b, Jean-Marc Fedeli^c, Pierrette Rivallin^c, Kavita Surana^c, and Lorenzo Pavesi^a

^aNanoscience Laboratory, Department of Physics, University of Trento, Via Sommarive 14, 38123 Povo (Trento), Italy

*tengattini@science.unitn.it, phone number: (+39) 0461/282941, fax number: (+39) 0461/282967

^bDepartament d'Electrònica, Universitat de Barcelona, Carrer Martí i Franquès 1, Barcelona 08028, Spain

^cCEA, Léti, Minatec campus 17 rue des Martyrs, 38054 Grenoble cedex 9, France

ABSTRACT

The convergence of photonics and microelectronics within a single chip is still lacking of a monolithical on-chip optical amplifier. Rare-earth doped slot waveguides show a large potential as on-chip source. Slot waveguides with silicon nanocrystals embedded in a dielectric host matrix can increase the light confinement in the active layer and allow electrical injection. In this work, horizontal slot waveguides formed by two thick silicon layers separated by a thin erbium doped silicon rich silicon oxide layer are studied as on-chip optical amplifiers. The waveguides are grown in a CMOS line with the active material grown by low-pressure chemical vapor deposition. Optical tests are performed and light propagation in the slot waveguides is observed. Using the cut-back technique, spectra propagation losses are evaluated. Room temperature electroluminescence is observed at 1.54 μm . Transmitted optical signal resonant with Er absorption is studied as a function of the injected current for different probing laser wavelengths.

Keywords: Integrated optics, silicon nanocrystals, erbium, slot waveguide, amplifier, electroluminescence

I. INTRODUCTION

The convergence of photonics and microelectronics within a single chip is still lacking of a monolithical on-chip optical amplifier. The remaining critical capability, which has yet to be demonstrated on the integrated silicon photonic platform using standard microelectronic fabrication processes, is electrically pumped amplification within a silicon waveguide¹. Silicon is, in fact, an excellent waveguide material because it is transparent in the telecommunications band ($\lambda = 1550$ nm), it has a high refractive index and can be processed inexpensively, but it is a poor light emitting material due to its indirect band gap. Therefore it is more convenient to combine a silicon waveguide structure with a more efficient 1550 nm gain material for on-chip applications. Even though electrically pumped lasers have been demonstrated with III-V materials evanescently coupled to a silicon waveguide², these approaches rely on a wafer bonding step, impeding a monolithically integration. At the same time, optically pumped lasing has been shown in erbium-doped oxide structures³, but electrical pumping of insulating materials is not straightforward.

One possible solution, towards the realization of an electrically pumped silicon based laser, is to use rare-earth doped slot waveguides⁴. This work will be focused on the electrically pumped silicon nanocrystals erbium doped slot waveguides. These structures increase the light confinement in the active layer, leading to a higher light-matter interaction.

1.1 Waveguide design

The devices studied in this work are horizontal slot waveguides. These waveguides are formed by two thick silicon layers separated by a thin erbium doped silicon rich silicon oxide (SRO) multilayer, where the light confinement is higher. The cross section of the device is shown in Figure 1, with a zoom on the active layer of the structure (Figure 1b). It has to be noted that this design is a compromise between the optical and the electrical performances. The active region of the devices is a SiO₂/SRO multilayered structure with a total thickness of 50 nm. This value is the maximum for which efficient electrical injection has been demonstrated⁵ and the optimum one for the minimum laser threshold⁶. Previous studies on light emitting devices (LEDs) were done in order to optimize the active material for these devices^{7, 8}.

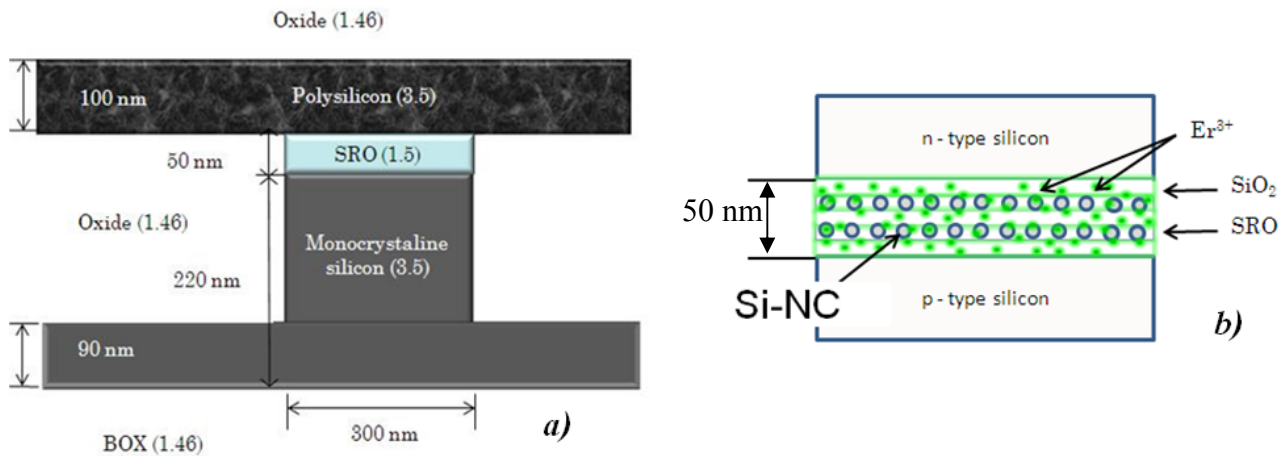


Figure 1. a) A schematic cross section of the erbium doped silicon slot waveguide. b) Zoom on the active layer of the device.

1.2 Active material waveguide fabrication

The samples are fabricated in a CMOS line, with the active material grown by using Low Pressure Chemical Vapor Deposition (LPCVD). After the deposition, all the samples are thermally treated to yield the phase separation, the silicon precipitation and the nanocrystals (Si-NCs) formation. The annealing treatment is equal for all the samples (900 °C for one hour). Then, the erbium ions are introduced in the active layer using ion implantation with a dose of 10¹⁵ atoms/cm² and energy equal to 20 keV. After the implantation, the samples are additionally annealed to recover implantation induced defects and to activate the implanted erbium ions. This second annealing treatment is performed at 800 °C for six hours. An additional sample with thermal silicon dioxide layer implanted with erbium ions is also fabricated in order to compare erbium doped slot waveguide with and without Si-NCs.

Table 1 reports a summary of the devices under study.

Table 1. Fabrication details of the devices under study. The digit in percent is the silicon excess content.

	P01	P02
<i>LPCVD Multilayer</i> ((2 nm 0% + 3 nm 20 %) x 10) + 2 nm 0 %	X	
<i>Thermal oxide</i> (50 nm)		X
Annealing at 900°C for one hour	X	X
Er implantation [dose: 10 ¹⁵ atoms/cm ² ; energy: 20keV]	X	X
Post – annealing at 800°C for six hours	X	X

II. OPTICAL CHARACTERIZATION

The light is coupled in and out from the erbium doped silicon slot waveguide by using gratings. The distance between the grating and the active part (i.e. the one Er doped) waveguide is 0.8 mm. Figure 2 shows the layout of these structures. An angular dependence study has been performed in order to find the optimum incident angle which maximizes the coupling efficiency. This study has been performed by using only one input grating and collecting the light from the output facet of the cleaved waveguide. As input, the signal is tuned in a region between 1.5 and 1.6 μm – the region of interest because of the erbium absorption and emission - while the output signal is split between a germanium photo detector and an infrared camera. In this way it is possible to have a quantitative value of the transmitted optical power and to see the optical mode at the same time. Figure 3 shows the transmitted intensity at a fixed wavelength of 1540 nm as a function of the incident angle (with respect to the normal). The angle, which maximizes the coupling between the input fiber and the slot waveguide, is 25°. It has to be noticed that, changing the coupling angle, the peak of the transmitted spectrum shifts in agreement with previous works^{9,10}.

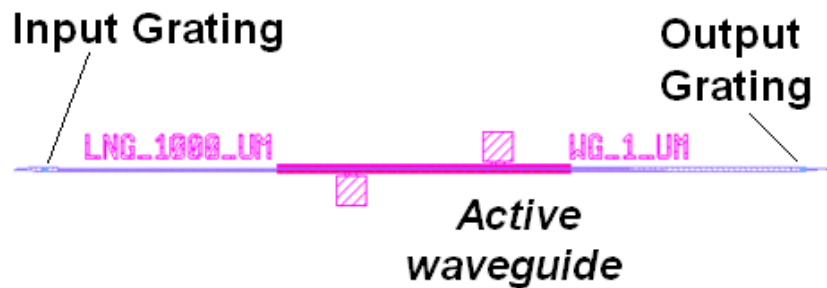


Figure 2. Layout of the test structure, which includes the two grating couplers, the adiabatic tapers, and the active waveguide (central purple part).

The transmission coefficient in a slot waveguide 1 mm long (lateral dimension 1 μm) is $T = -40$ dB. The grating selectively couples only to the TM polarization.

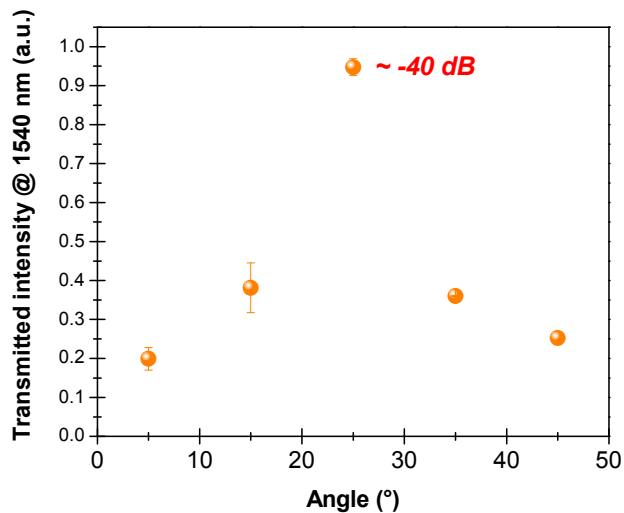


Figure 3. Transmitted intensity at 1540 nm as a function of the incident angle.

The propagation losses of the erbium doped slot waveguides are then calculated from the transmitted intensities of structures with different lengths (1, 2 and 3 mm, width 1 μm), using both gratings. The measurements have been performed at different laser wavelengths in a range between 1300 and 1600 nm, in order to evaluate the propagation losses of the waveguide and study the role of the silicon nanocrystals and of the erbium ions. The coupling losses are different too, because the structure is optimized for guiding the light with a wavelength near to the erbium emission region. Figure 4 shows the transmitted power as a function of the waveguide length for five different wavelengths, while Table 2 summarizes the evaluated propagation losses. The coupling losses are higher for the wavelength equal to 1300 and 1600 nm, as expected.

As shown in the figure 4, there is not a clear dependence of the propagation losses as a function of the different wavelengths. The erbium ion absorption is masked by the high measured propagation losses. The estimated absorption of erbium should be around 6 dB/cm and in this case it can be covered by the different statistical error of the measurements.

From similar measurements performed on waveguides P02, comparable values of propagation losses have been found, while coupling losses are higher. This result leads to the conclusion that the losses are mainly due to the waveguide itself, and not to the active layer.

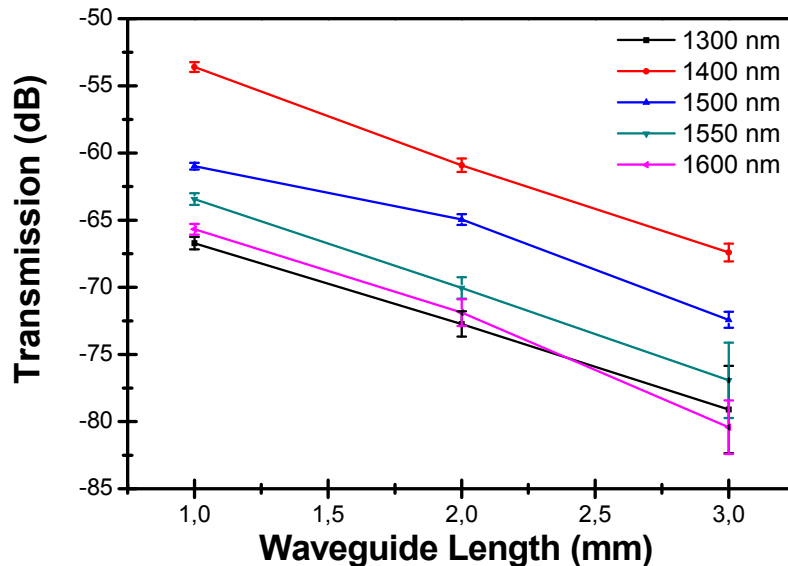


Figure 4. Transmitted power as a function of the slot waveguide length and the laser wavelength.

Table 2. Summary of the propagation losses at different wavelengths for P01.

Wavelength (nm)	Propagation losses (dB/cm)
1300	61 ± 1
1400	70 ± 2
1500	52 ± 9
1550	67 ± 1
1600	68 ± 6

III. ELECTRICAL CHARACTERIZATION

An electrical characterization of the device has been performed on the different active layers. Current-voltage (I-V) characteristics are recorded with a semiconductor device analyzer and are studied in order to see the conductivity of the three different active layers. Figure 5 shows the I-V characteristics for all the three layers under study, for a waveguide 1 mm long (with lateral dimension of 1 μm). The plot spans a voltage range between -20 and -40 V, when the device is in forward bias (accumulation regime). In this configuration, the current flux is obviously higher than in the depletion regime. For P02, the samples without Si-NCs, higher voltage (up to 50 V) can be achieved in forward bias without breaking the device.

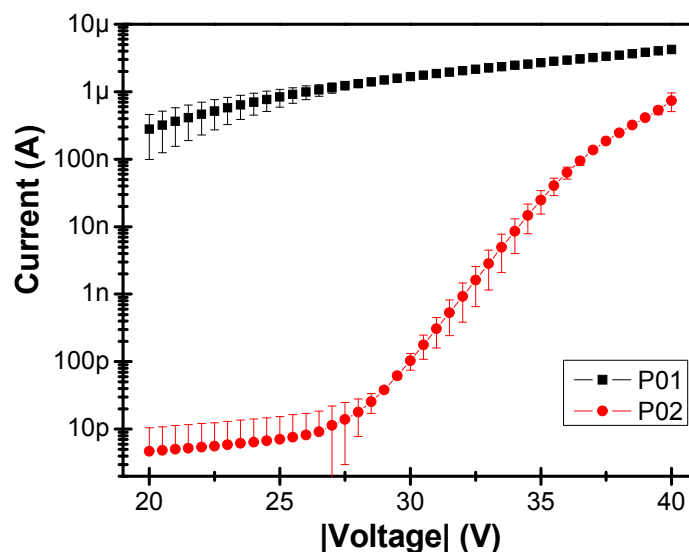


Figure 5. I-V curves for the two different active layers.

As can be observed in the figure, P02 presents resistivity higher than P01. The presence of the silicon nanocrystals in the active layer of the device leads to a higher conductivity, an improvement in the fabrication reproducibility and a long-term stability of the devices. All these facts have already been observed in light emitting diodes (LEDs) with the same active material.

IV. OPTO-ELECTRICAL CHARACTERIZATION

This section is divided into two parts: first, a study of the transmitted power at different probing wavelengths is reported, and then the electroluminescence is studied.

4.1 Transmission measurements

Propagation losses are measured as a function of the applied bias voltage/current. Increased attenuation is observed, probably due to the free-carrier absorption phenomena (FCA). Figure 6 shows the signal enhancement (SE) factor, which is defined as the ratio between the intensity of the signal transmitted when the waveguide is electrically pumped (I_{p-p}) and the intensity of the signal when the waveguide is not pumped (I_{probe}).

$$SE = 10 * \log \frac{I_{p-p}}{I_{probe}} \quad [\text{dB}]$$

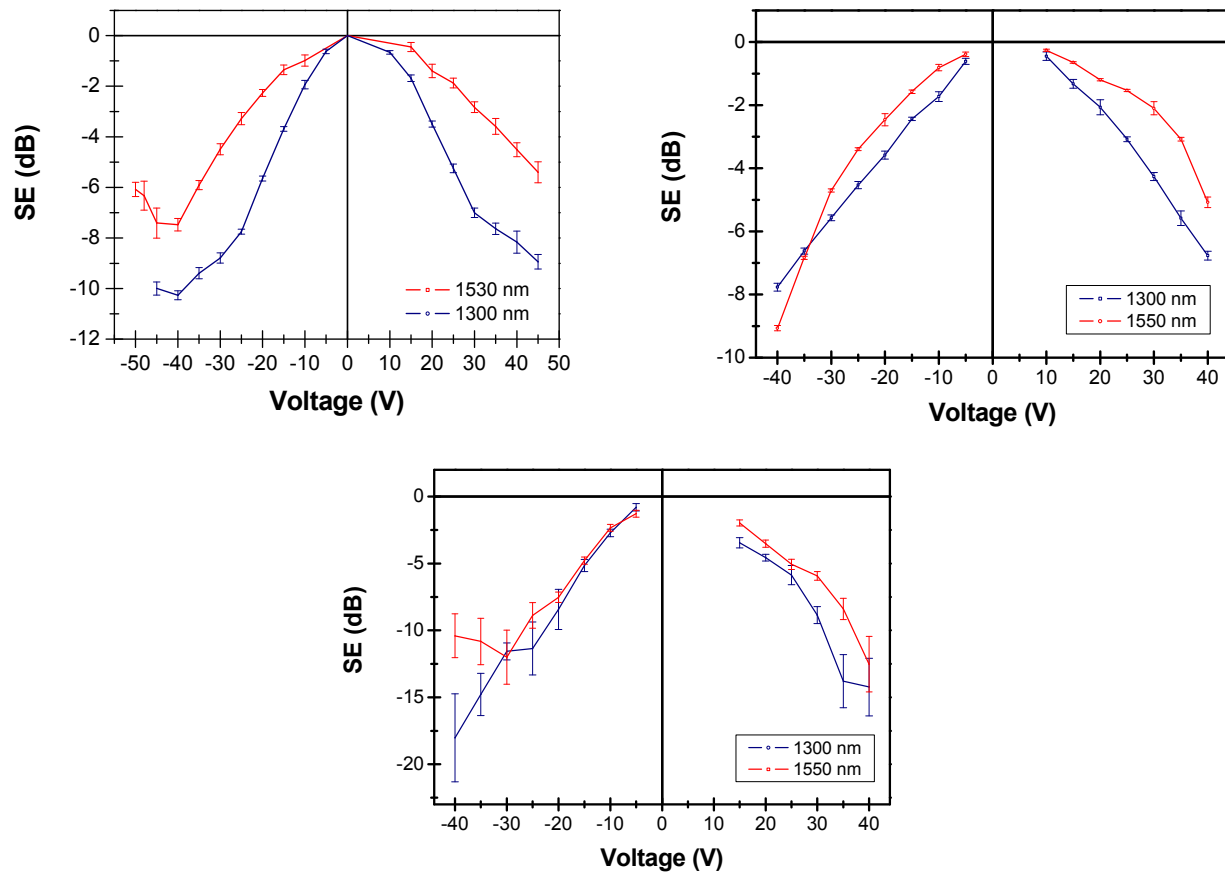


Figure 6. SE as a function of the voltage for a 1 mm long waveguide on P02 (top-left) and on P01 (top-right), and for a waveguide 3 mm long on P01 (bottom). All the analyzed waveguides are 1 μm wide. The negative applied voltage corresponds to forward bias polarization, while the positive applied voltage to reverse bias polarization.

Let us note that for all the biases the transmission is reduced with respect to the zero bias value. This is due to free carrier absorption (FCA) losses caused by the injected current in the silicon slot waveguide. Moreover, the losses are higher in forward bias than in reverse bias, because the injected electron current is higher, too, as discussed in the previous section. At the same time it is interesting to note that the attenuation is higher for a signal at 1300 nm. This behavior is in agreement with the weak dependence of the FCA cross section from the probing wavelength¹¹.

Comparing the results for the 1 mm long waveguides, it is evident that the SE is lower for P01 than for P02 at high applied voltages (larger than 35 V). The propagation losses due to FCA¹² are roughly 90 dB/cm for P01 and 75 dB/cm for P02, at $V = -40$ V at a wavelength of 1550 nm.

Very interestingly, in the 3 mm long P01 waveguide and in all the P02 waveguides, the behavior of SE is not monotonic but at higher injection rate it starts to increase. Since this injection range is also that characteristics of electroluminescence emission (see more later) it is possible that this is due to the active role of erbium ions which counteracts the FCA. Note that due to the small thickness of the Er doped region, the optical confinement factor in this region is small. This absorption bleaching (or internal gain) is observed at voltages higher than 40 V for P02. This same effect can be observed in P01, but only for the longest waveguide (see Figure 6 – bottom part). The spectral dependence of the signal enhancement has been measured, but the noisy signal does not allow to see a clear similarity to the Er emission spectrum.

4.2 Electroluminescence

Electroluminescence (EL) has been collected with a tapered fiber from the grating, with an angle of 25° with respect to the normal. In this configuration, without the probing laser, the emitted light is very weak and high biasing voltages are needed (higher than 40 V) to actually collect a detectable signal. This light is detected with an infrared avalanche photo diode (APD), while the current is forced with a semiconductor parameter analyzer. Figure 7 shows the EL dependence as a function of the injected current. The data shown referred to a waveguide 1 mm long and with lateral dimension of $1\ \mu\text{m}$. It has to be noticed that P02 shows higher electroluminescence signal in respect to P01. This fact is in accordance with what found in LEDs with the same active material.

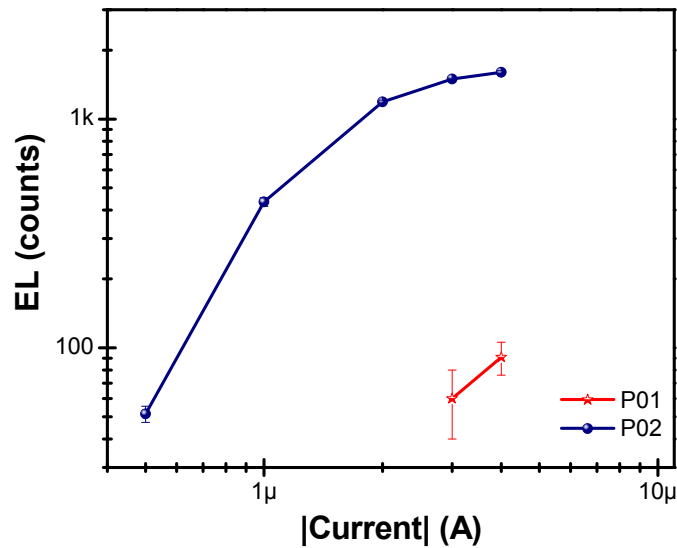


Figure 7. Electroluminescence signal as a function of the injected current in the accumulation regime for P01 and P02.

Finally, EL was measured on several devices with different lengths. It seems that there is no clear dependence of the collected signal as a function of the waveguide length, suggesting that the light emitted from the erbium ions is immediately lost. This is not surprising since the very high propagation losses measured in the waveguide. The light collected comes simply in the active region closest to the grating. At the same time, however, care was taken to be sure that the EL collected was actually coming from the waveguide itself and not from spurious reflections.

V. CONCLUSIONS

Erbium doped slot waveguides, which have as active region erbium ions with or without silicon nanocrystals, were designed and fabricated. Optical tests are performed and high propagation losses are found in all the samples. This result leads to the conclusion that the losses are mainly due to the waveguide itself, and not to the active layer. Electrical tests and opto-electrical measurements show that it is possible to have electroluminescence light and that the losses increase when an injected current is flowing into these devices. The electroluminescence is mainly due to the impact excitation of the Er ions, while, on the contrary, the signal attenuation is due to free-carrier absorption and charge accumulation. At high voltages, i.e. high injected current, we observed absorption bleaching, which can be optimistically interpreted as due the positive role played by stimulated emission in the Er ions.

The table 3 summarizes the results obtained for both P01 and P02.

	P01	P02
<i>Electrical characterization</i>	<ul style="list-style-type: none"> • Low resistivity • $V_{\text{breakdown}} \sim 42 \text{ V}$ 	<ul style="list-style-type: none"> • High resistivity • $V_{\text{breakdown}} \sim 50 \text{ V}$
<i>Optical characterization</i>	High propagation losses	High propagation losses High coupling losses
<i>Electro-Optical characterization</i>	<ul style="list-style-type: none"> ▪ Weak electroluminescence ▪ Absorption bleaching for the longest waveguide 	<ul style="list-style-type: none"> ▪ Strong electroluminescence ▪ Absorption bleaching for all the waveguides

Finally, from these measurements, it seems that the high working voltage, the high propagation losses and the free carrier absorption effect prevent the demonstration of a working optical amplifier. However, the presence of light emission from erbium ions and the absorption bleaching of the transmitted signal at high injected currents/high voltages leave some hopes that an actual Er doped amplifier can be finally fabricated.

ACKNOWLEDGMENTS

This work has been supported by the European Commission through the project ICT-FP7-224312 HELIOS.

REFERENCES

- [1] Pavesi L., "Silicon-Based Light Sources for Silicon Integrated Circuits", Advances in Optical Technologies, Volume 2008, (2008).
- [2] Van Campenhout J., Rojo Romeo J., Regreny P., Seassal C., Van Thourhout D., Verstuyft S., Di Cioccio L., Fedeli J.-M., Lagahe C., and Baets R., "Electrically pumped InP-based microdisk lasers integrated with a nanophotonic silicon-on-insulator waveguide circuit", Optics Express, Vol. 15, Issue 11, pp. 6744-6749, (2007).
- [3] Polman A., Min B., Kalkman J., Kippenberg J., and Vahala K. J., "Ultralow-threshold erbium-implanted toroidal microlaser on silicon", Applied Physics Letters, Vol. 84, pp. 1037-1039, (2004).
- [4] Ramirez J.M., Ferrarese Lupi F., Jambois O., Berencen Y., Navarro-Urrios D., Anopchenko A., Marconi A., Prtljaga N., Tengattini A., Pavesi L., Colonna J. P., Fedeli J.-M., and Garrido B., "Erbium emission in MOS light emitting devices: from energy transfer to direct impact excitation", Nanotechnology, Vol. 23, (2012).
- [5] Marconi A., Anopchenko A., Wang M., Pucker G., Bellutti P., and Pavesi L., "High power efficiency in Si-nc/SiO₂ multilayer light emitting devices by bipolar direct tunneling", Applied Physics Letters, Vol. 94, 221110, (2009).
- [6] Robinson J. T., Preston K., Painter O., and Lipson M., "First-principle deviation of gain in high-index contrast waveguides", Optics Express, Vol. 16, Issue 21, pp. 16659-16669, (2008).
- [7] Tengattini A., Marconi A., Anopchenko A., Prtljaga N., Ramirez, J.M., Jambois O., Berencen Y., Navarro-Urrios D., Garrido B., Milesi F., Colonna J., Fedeli J.-M., and Pavesi L., "1.54 μm Er doped light emitting devices: the role of the silicon content", Proc. IEEE Group IV Photonics (GFP), pp. 77-79, (2011).
- [8] Anopchenko A., Tengattini A., Marconi A., Prtljaga N., Ramirez J. M., Jambois O., Berencen Y., Navarro-Urrios D., Garrido B., Milesi F., Colonna J.-P., Fedeli J.-M., and Pavesi L., "Bipolar pulsed excitation of erbium-doped nanosilicon light emitting diodes", Journal of Applied Physics, Vol. 111, 063102, (2012).
- [9] Lockwood D. J., and Pavesi L., [Silicon Photonics II], Springer-Verlag Berlin Heidelberg, Chapter 3, pp. 71-76, (2011).
- [10] Taillaert D., Van Laere F., Ayre M., Bogaerts W., Van Thourhout D., Bientman P., and Baets R., "Grating Couplers for Coupling between Optical Fibers and Nanophotonic Waveguides", Japanese Journal of Applied Physics, Vol. 45, Issue 8A, pp. 6071-6077, (2006).
- [11] Soref R. A., and Bennett B. R., "Electro optical effects in silicon", IEEE Journal of Quantum Electronics, Vol. 23, N. 1, pp. 123-129, (1987).
- [12] Navarro-Urrios D., Pitanti A., Daldosso N., Gourbilleau F., Rizk R., Pucker G., and Pavesi L., "Quantification of the carrier absorption losses in Si-nanocrystal rich rib waveguides at 1.54 μm ", Applied Physics Letters, Vol. 92, 051101, (2008).